

# Q-switched induced gain switching of a two-transition cascade laser

Jianfeng Li,<sup>1,2,\*</sup> Tomonori Hu,<sup>1</sup> and Stuart D. Jackson<sup>1</sup>

<sup>1</sup>Institute of Photonics and Optical Science and the Centre for Ultrahigh Bandwidth Devices for Optical Systems (CUDOS), School of Physics, University of Sydney, Camperdown 2006, Australia

<sup>2</sup>State Key Laboratory of Electronic Thin Films and Integrated Devices, School of Optoelectronic Information, University of Electronic Science and Technology of China (UESTC), Chengdu 610054, China

\*ljianfeng@uestc.edu.cn

**Abstract:** A gain-switched laser transition, of a two-laser-transition cascade laser, that is driven by the adjacent laser transition which is Q-switched is demonstrated using a Ho<sup>3+</sup>-doped fluoride fiber laser. Q-switching the <sup>5</sup>I<sub>6</sub> → <sup>5</sup>I<sub>7</sub> transition at 3.002 μm produces stable gain-switched pulses from the <sup>5</sup>I<sub>7</sub> → <sup>5</sup>I<sub>8</sub> transition at 2.074 μm; however, Q-switching the <sup>5</sup>I<sub>7</sub> → <sup>5</sup>I<sub>8</sub> transition produced multiple gain switched pulses from the <sup>5</sup>I<sub>6</sub> → <sup>5</sup>I<sub>7</sub> transition. The gain-switched pulses were measured to be of a similar duration to the Q-switched pulses suggesting that much shorter pulses of closer duration could be generated at pump power higher levels.

©2012 Optical Society of America

OCIS codes: (140.3510) Lasers, fiber; (140.3480) Lasers, diode-pumped.

---

## References and links

1. K. Y. Lau, "Gain switching of semiconductor injection lasers," *Appl. Phys. Lett.* **52**(4), 257–259 (1988).
2. Y. Arakawa, T. Sogawa, M. Nishioka, M. Tanaka, and H. Sakaki, "Picosecond pulse generation (<1.8 ps) in a quantum well laser by a gain switching method," *Appl. Phys. Lett.* **51**(17), 1295–1297 (1987).
3. S. D. Jackson and T. A. King, "Efficient gain-switched operation of a Tm-doped silica fiber laser," *IEEE J. Quantum Electron.* **34**(5), 779–789 (1998).
4. M. Jiang and P. Tayebati, "Stable 10 ns, kilowatt peak-power pulse generation from a gain-switched Tm-doped fiber laser," *Opt. Lett.* **32**(13), 1797–1799 (2007).
5. B. Schmaul, G. Huber, R. Clausen, B. Chai, P. Li Kam Wa, and M. Bass, "Er<sup>3+</sup>:YLiF<sub>4</sub> continuous wave cascade laser operation at 1620 and 2810 nm at room temperature," *Appl. Phys. Lett.* **62**(6), 541–543 (1993).
6. R. M. Percival, D. Szebesta, and S. T. Davey, "Highly efficient CW cascade operation of 1.47 and 1.82 μm transitions in Tm-doped fluoride fiber laser," *Electron. Lett.* **28**(20), 1866–1868 (1992).
7. G. Qin and Y. Ohishi, "Cascaded two-wavelength lasers and their effects on C-Band amplification performance for Er<sup>3+</sup>-doped fluoride fiber," *IEEE J. Quantum Electron.* **43**(4), 316–321 (2007).
8. M. Pollnau, Ch. Ghisler, G. Bunea, M. Bunea, W. Lüthy, and H. P. Weber, "150 mW unsaturated output power at 3 μm from a single-mode-fiber erbium cascade laser," *Appl. Phys. Lett.* **66**(26), 3564–3566 (1995).
9. J. Schneider, "Fluoride fiber laser operating at 3.9 μm," *Electron. Lett.* **31**(15), 1250–1251 (1995).
10. T. Sumiyoshi, H. Sekita, T. Arai, S. Sato, M. Ishihara, and M. Kikuchi, "High-power continuous-wave 3- and 2-μm cascade Ho<sup>3+</sup>:ZBLAN fiber laser and its medical applications," *IEEE J. Sel. Top. Quantum Electron.* **5**(4), 936–943 (1999).
11. J. Schneider, "Mid-infrared fluoride fiber lasers in multiple cascade operation," *IEEE Photon. Technol. Lett.* **7**(4), 354–356 (1995).
12. M. Pollnau, Ch. Ghisler, W. Lüthy, H. P. Weber, J. Schneider, and U. B. Unrau, "Three-transition cascade erbium laser at 1.7, 2.7, and 1.6 microm," *Opt. Lett.* **22**(9), 612–614 (1997).
13. S. D. Jackson, M. Pollnau, and J. Li, "Diode pumped erbium cascade fiber lasers," *IEEE J. Quantum Electron.* **47**(4), 471–478 (2011).
14. J. Li, D. D. Hudson, and S. D. Jackson, "High-power diode-pumped fiber laser operating at 3 μm," *Opt. Lett.* **36**(18), 3642–3644 (2011).

---

## 1. Introduction

Gain switching is a convenient pulse generation technique allowing the generation of pulses with pulse durations spanning at least 6 orders of magnitude. As opposed to Q-switching which involves modulating the fractional power loss per round trip, switching the gain of laser transition, a traditional pulsing technique going back to the first demonstrations of lasers, involves directly modulating the population in the energy levels comprising the population

inversion independent of the loss of the cavity. By modulating the injection current of semiconductor diode lasers [1] for example, short pulses, down to a few ps duration, can be generated [2] and more recently, using optical pump pulses to excite fiber lasers [3] the generation pulses of a few ns duration [4] has been demonstrated.

Cascade lasing of rare earth ion transitions allows the generation of a number of distinct emission wavelengths simultaneously, which may be an effective method to create power-scaled mid-infrared fiber lasers. Cascading lasing at 2.81  $\mu\text{m}$  and 1.62  $\mu\text{m}$  from  $\text{Er}^{3+}$  crystalline lasers [5] for example relies on host materials that support less energetic phonons so that adjacent electronic transitions have sufficient luminescence efficiencies to allow a lasing threshold for each transition at a comparable level of pump power. To date, cascade lasing of fiber lasers has relied on low phonon energy fluoride glasses which are capable of supporting fluorescence from the near infrared [6,7] to the mid-infrared [8–10] and cascade lasing on up to three transitions has been demonstrated [11,12]. Cascade lasing reduces the thermal load by creating large photon conversion efficiencies which is particularly important in low phonon glasses which typically have relatively poor thermo-mechanical characteristics [13].

In this paper, we demonstrate a new gain-switching process whereby modulation of the population inversion of a transition is produced from the forced modulation of an adjacent transition of a two transition cascade. We show using cascade lasing of a  $\text{Ho}^{3+}$ -doped fluoride fiber laser at 3  $\mu\text{m}$  and 2.1  $\mu\text{m}$ , that by Q-switching one transition of the cascade, the energy levels of the adjacent transition are sufficiently modulated to cause gain-switched pulsing. Gain-switched pulses of a similar duration to the Q-switched pulses can be produced with a time delay between pulses that is dependent on the pump power and repetition rate of the Q-switch.

## 2. Experiment setup

The experimental setup is shown in Fig. 1. Commercial high power at 1.15  $\mu\text{m}$  diode lasers (Ferdinand-Braun-Institut für Höchstfrequenztechnik, Berlin) were used to pump each end of the double clad  $\text{Ho}^{3+}$ -doped fluoride fiber after polarization multiplexing using a standard polarizing beam cube and focusing using two ZnSe objective lenses (Innovation Photonics, LFO-5-6-5, 0.25 NA) which also collimated the  ${}^5\text{I}_6 \rightarrow {}^5\text{I}_7$  and  ${}^5\text{I}_7 \rightarrow {}^5\text{I}_8$  laser transition outputs from the fiber core. Two highly pump-transmitting dichroic mirrors with 60% reflectivity between 2.0  $\mu\text{m}$  and 2.1  $\mu\text{m}$  and >98% reflectivity between 2.5  $\mu\text{m}$  and 3.2  $\mu\text{m}$  were each positioned between the polarizing beam splitter and focusing lens at angle of  $15^\circ$  with respect to the pump beam. One dichroic mirror was used to steer the laser output onto a  $\text{TeO}_2$  acousto-optic modulator (AOM) that had a rise of 115 ns; the other mirror was used to outcouple the fiber laser output. The AOM with 89% transmission in the 2.1  $\mu\text{m}$  region and 86% transmission in the 3  $\mu\text{m}$  region was placed into the external cavity of the fiber laser in a first-order diffraction mode arrangement. The measured diffraction efficiencies were 82% and 83% for the 2.1  $\mu\text{m}$  and 3  $\mu\text{m}$  emissions, respectively. To produce  ${}^5\text{I}_6 \rightarrow {}^5\text{I}_7$  output or  ${}^5\text{I}_7 \rightarrow {}^5\text{I}_8$  output simultaneously when its cascade laser operates in the Q-switching state, the fiber end with respect to the AOM was cleaved perpendicularly to form a Fresnel-reflection-based cavity. The  $\text{Ho}^{3+}$ -doped double clad fluoride fiber (FiberLabs, Japan) was identical to the fiber used in our previous free-running experiment [14] and had a D-shaped cladding with a diameter of 125  $\mu\text{m}$  and a numerical aperture (NA) of 0.50. The core was 10  $\mu\text{m}$  in diameter, had an NA of 0.16 and was doped with 1.2 mol%  $\text{Ho}^{3+}$ ; the fiber length of 11.0 m provided 98% pump absorption efficiency. A gold-coated plane ruled grating (600 lines per mm, blaze angle  $\theta_B = 17.5^\circ$ ) was used to separate the two cascaded transitions. Two InAs photodiodes (response time of  $\sim 10$  ns) and a 100 MHz oscilloscope (Tektronix TDS1012) were used to measure the pulse characteristics. An optical spectrum analyzer (Yokogawa AQ6375, Japan) was used to measure the spectrum at 2.1  $\mu\text{m}$  and the spectrum at 3  $\mu\text{m}$  was measured using a calibrated monochromator with 0.3 nm resolution.

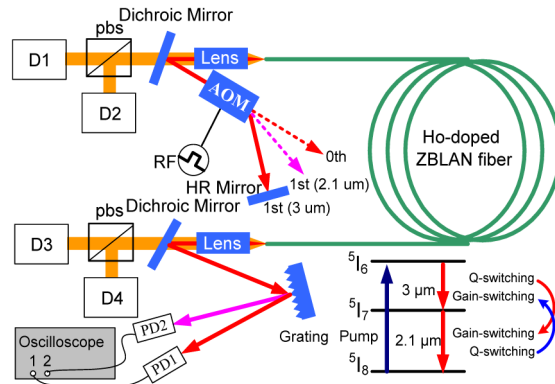


Fig. 1. Schematic of the experimental setup. D1-D4 represents the pump diodes, pbs the polarizing beam splitter and PD1 and PD2 represent the photo detector. Included is a simplified energy level diagram of the Ho<sup>3+</sup> ion showing the gain-switching transition driven by the adjacent Q-switched laser transition.

### 3. Results and discussion

The first-order diffracted light from the  ${}^5I_6 \rightarrow {}^5I_7$  transition was first fed back into the cavity and, by adjusting the repetition frequency of the AOM and pump power, stable pulses arising from the  ${}^5I_6 \rightarrow {}^5I_7$  transition were generated, see Fig. 2, which was measured at the repetition rate of 30 kHz for the maximum launched pump power of 7.4 W. The Q-switched fiber laser operated at a slope efficiency of 12.7% and threshold of 300 mW. The pulse had a duration of 350 ns (FWHM), 21.7 μJ pulse energy and peak power of 62 W. After a time delay of ~2.2 μs, a gain-switched pulse train from the  ${}^5I_7 \rightarrow {}^5I_8$  transition was generated. The total gain-switched output from both fiber ends operated at a slope efficiency of 4.8% and threshold of 3.4 W and the pulse duration, pulse energy and peak power at maximum launched pump power were 460 ns, 6.4 μJ and 13.9 W, respectively. The gain-switched pulse was approximately 31% longer than the Q-switched pulse which indicates that the mechanism for gain switching is directly related to the Q-switched pulse; the population in the  ${}^5I_7$  level was modulated at the Q-switched pulse generation rate. The gain-switched pulse quickly depopulated the  ${}^5I_7$  level excitation replenishing ground states and therefore ground state absorption (GSA). The pulse-to-pulse stability for both the Q-switched and gain-switched pulses was approximately  $\pm 10\%$ .

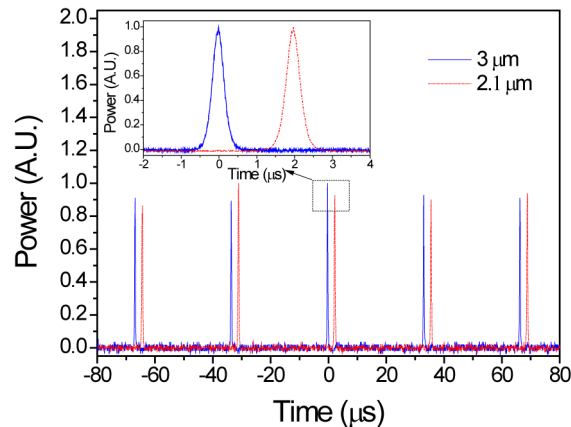


Fig. 2. Synchronized output pulse trains for the Q-switched  ${}^5I_6 \rightarrow {}^5I_7$  pulse and the gain-switched  ${}^5I_7 \rightarrow {}^5I_8$  pulse at the repetition rate of 30 kHz for the maximum launched pump power of 7.4 W. The inset shows the temporal pulse waveform for  ${}^5I_6 \rightarrow {}^5I_7$  and  ${}^5I_7 \rightarrow {}^5I_8$  transitions.

Figure 3 shows the repetition rates providing stable pulse generation and the corresponding pulse widths of the pulses for each transition at three launched pump powers. The gain-switched pulses were generated at the same repetition rate as the Q-switched pulses; multiple Q-switch and gain-switch pulsing occurred when the repetition rate of the AOM was lower than 30 kHz; unstable pulsing occurred when the repetition rate of the AOM was larger than 70 kHz. The width of the Q-switched and gain-switched pulses shortened with increasing pump power and lengthened significantly with increasing repetition rate. The inset to Fig. 3 shows the time delay,  $\Delta t$ , between the Q-switched and gain-switched pulses as a function of repetition rate and launched pump power. The time delay decreases and increases near linearly with the launched pump power and repetition rate, respectively. The shortest time delay of 2.2  $\mu\text{s}$  occurred at a repetition rate of 30 kHz and at maximum launched pump power.

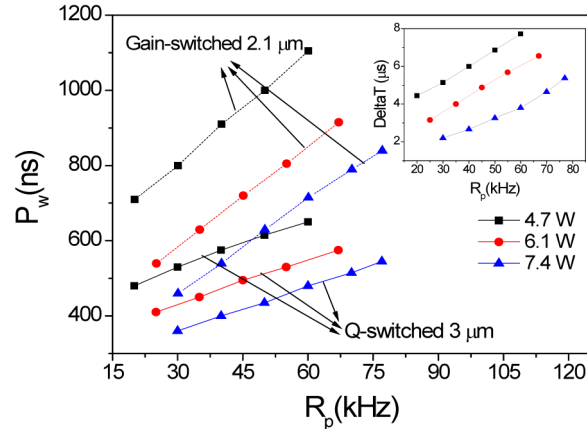


Fig. 3. Measured pulse width,  $P_w$ , of the  $^5\text{I}_6 \rightarrow ^5\text{I}_7$  and  $^5\text{I}_7 \rightarrow ^5\text{I}_8$  transitions as a function of the repetition rate,  $R_p$ , at three launched pump powers. The inset shows the time delay,  $\Delta t$ , between  $^5\text{I}_6 \rightarrow ^5\text{I}_7$  and  $^5\text{I}_7 \rightarrow ^5\text{I}_8$  pulses as a function of  $R_p$  at three launched pump powers.

Figure 4 shows the output pulses for first-order Q-switching of the  $^5\text{I}_7 \rightarrow ^5\text{I}_8$  transition and the resultant gain-switched pulses generated from the  $^5\text{I}_6 \rightarrow ^5\text{I}_7$  transition; the inset to Fig. 4 shows the characteristics of each pulse at a repetition rate of 30 kHz and at maximum launched pump power. The Q-switched ( $^5\text{I}_7 \rightarrow ^5\text{I}_8$ ) pulse operated at a slope efficiency of 4.0% and threshold of 2.8 W had pulse duration of 300 ns, pulse energy of 6.1  $\mu\text{J}$  and a peak power of 20.4 W. After a time delay of 9.8  $\mu\text{s}$ , multiple gain-switched ( $^5\text{I}_6 \rightarrow ^5\text{I}_7$ ) pulses were measured for all values of the repetition rate of the AOM. The gain-switched pulse durations were 720 ns, nearly twice the duration of the Q-switched pulse. The repetition rate providing stable Q-switched ( $^5\text{I}_7 \rightarrow ^5\text{I}_8$ ) pulses was 17 kHz to 47 kHz. The number of gain-switched pulses and time between them decreased with increasing repetition rate. The duration of the gain-switched and Q-switched pulses shortened with increasing pump power and increased with increasing repetition rate; the narrowest Q-switched and gain-switched pulse widths were 270 ns and 640 ns, respectively which was achieved at 17 kHz and 7.4 W launched pump power. The characteristics of the time delay between Q-switched and gain switched pulses was identical to the alternative switching arrangement; the shortest time delay of 7.6  $\mu\text{s}$  was observed at 17 kHz and 7.4 W launched pump power.

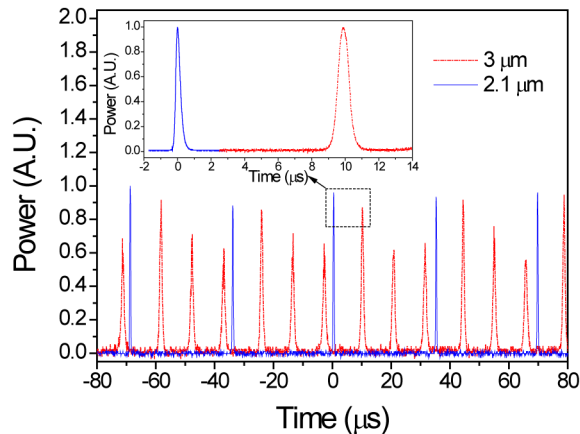


Fig. 4. Synchronized output pulse trains for the Q-switched  ${}^5I_7 \rightarrow {}^5I_8$  pulse and gain-switched  ${}^5I_6 \rightarrow {}^5I_7$  pulse for the maximum launched pump power of 7.4 W. The inset shows the temporal pulse waveform for  ${}^5I_6 \rightarrow {}^5I_7$  and  ${}^5I_7 \rightarrow {}^5I_8$  transitions.

The optical spectrum of the output at the maximum launched pump power for the Q-switched pulses and the corresponding gain-switched pulses is shown in Fig. 5. The Q-switched pulses arising from  ${}^5I_6 \rightarrow {}^5I_7$  ( ${}^3I_7 \rightarrow {}^5I_8$ ) transition operated with a center wavelength of  $3.002 \mu\text{m}$  ( $2.074 \mu\text{m}$ ) and bandwidth of 16 nm (4.5 nm), while the gain-switched pulses arising from  ${}^5I_6 \rightarrow {}^5I_6$  ( ${}^3I_7 \rightarrow {}^5I_8$ ) transition operated with a center wavelength of  $2.986 \mu\text{m}$  ( $2.072 \mu\text{m}$ ) and bandwidth of 13 nm (4 nm). The centre wavelength of the Q-switched pulse of a transition is longer than the corresponding gain-switched pulse of the same transition; the spectra of the Q-switched pulses are also broader. The gain-switched pulses were generated from cavities using feedback of approximately 4% Fresnel reflection that forces a higher threshold than the corresponding cavity generating Q-switched pulses. Thus the gain-switched transitions have a larger population inversion at threshold which allows the terminating Stark sub-level to be deeper in the lower laser level thus creating shorter emission wavelengths.

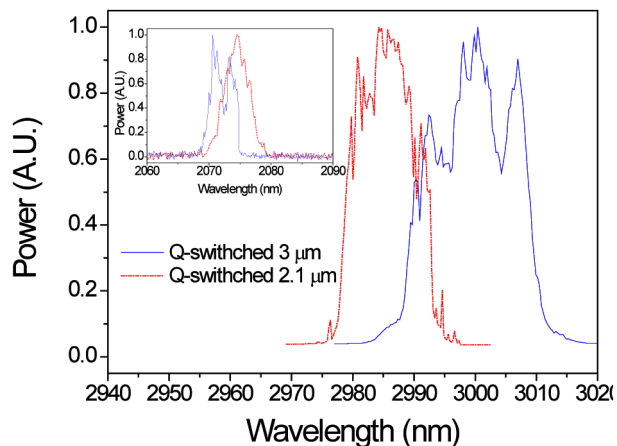


Fig. 5. Measured spectrum of the  ${}^5I_6 \rightarrow {}^5I_7$  laser transition at maximum pump power. The inset shows the measured spectrum for the  ${}^5I_7 \rightarrow {}^5I_8$  laser transition at maximum pump power.

A gain-switched pulse has been produced by a Q-switched pulse of the adjacent transition of a two transition cascade. The gain-switched pulses from the lower transition rely on the excitation of the upper laser level from the emission of the Q-switched higher transition pulse. This process is fast which results in a single gain-switched pulse of similar duration to the Q-switched pulse. On the other hand, when the lower transition is Q-switched, the process of

gain-switching the higher transition is more complicated. The upper laser level of the higher transition is continuously excited from the diode pump source; however the de-excitation of the lower laser level relies on the generation of the Q-switched pulse. After the generation of the lower transition Q-switched pulse, GSA is increased this creates greater localized excitation of the  $^5I_6$  level feeding the gain-switched pulse. There exists, therefore, a complex interplay between the excitation of the energy levels and pulse generation; we are currently constructing a numerical model to understand and further optimize this pulse generation technique. This mechanism can be transferred to passively Q-switched and mode-locked cascade lasers.

#### **4. Conclusion**

In this paper we have demonstrated the Q-switched pulse induced gain switching in a two-transition cascade laser. Using a  $\text{Ho}^{3+}$ -doped ZBLAN fibre laser that was pumped with high power CW diode lasers emitting at 1.15  $\mu\text{m}$  and operated cascade on two adjacent transitions emitting at 3  $\mu\text{m}$  and 2.1  $\mu\text{m}$ , gain-switched pulses as short as 460 ns at 2.07  $\mu\text{m}$  were created from 350 ns Q-switched pulses at 3.002  $\mu\text{m}$ . With optimized fibre and cavity parameters in conjunction with increased pumping, shorter pulses are envisaged. The pulse generation mechanism has potential applications in mid-infrared photonics and nonlinear optics.

#### **Acknowledgments**

The authors acknowledge financial support from the Australian Research Council through the Discovery Projects and Centre of Excellence funding schemes. SJ acknowledges support from a Queen Elizabeth II Fellowship. This work was also supported by National Nature Science Foundation of China (Grant No. 61107037 and 60925019), China Postdoctoral Science Special Foundation (Grant No. 201003693).